Int. J. Electrochem. Sci., 12 **(2017)** 10763 – 10772, doi: 10.20964/2017.11.63

International Journal of
ELECTROCHEMICAL
SCIENCE
www.electrochemsci.org

Synthesis of $MnCo_2O_{4.5}$/graphene Composite as Electrode Material for Supercapacitors

Yanhua Li, Xiahui Peng[*]*, Jialian Xiang, Jiaxin Yang*

Hunan Province Key Laboratory of Applied Environmental Photocatalysis, Changsha University, Changsha 410022, China
[*]E-mail: pxiahui630527@126.com

Received: 31 July 2017 / *Accepted:* 12 September 2017 / *Published:* 12 October 2017

$MnCo_2O_{4.5}$/graphene composite is obtained by a simple hydrothermal method. The as-synthesized $MnCo_2O_{4.5}$/graphene composite is characterized by X-ray diffraction, and scanning electron microscopy. Electrochemical property of $MnCo_2O_{4.5}$/graphene composite is carried out by cyclic voltammetry, galvanostatic charge-discharge and electrochemical impedance spectroscopy. $MnCo_2O_{4.5}$/graphene composite exhibits good supercapacitive performance. The specific capacitances of $MnCo_2O_{4.5}$/graphene composite at 5 mV s^{-1} and at 0.5 A g^{-1} are 255.8 and 252.3 F g^{-1}, respectively. 88.7% of the specific capacitance is retained for a 16-time current density increase, indicating its superior rate capability. At the 1000th cycle, $MnCo_2O_{4.5}$/graphene composite shows a specific capacitance of 225.6 F g^{-1} at 1.0 A g^{-1}, which is 92.6% of initial specific capacitance, demonstrating its excellent cycling stability. These characteristics illustrate that $MnCo_2O_{4.5}$/graphene composite is a promising electrode material in supercapacitors.

Keywords: Supercapacitors, $MnCo_2O_{4.5}$, Graphene , Hydrothermal method

1. INTRODUCTION

As electrochemical energy-storage devices, supercapacitors possess higher power density, faster charge-discharge rate and longer lifespan compared with batteries. These predominant advantages make supercapacitors suitable for applications in hybrid vehicles, portal electronics, and power back-ups [1, 2]. The properties of supercapacitors mainly depend on the properties of electrode materials. Up to now, a variety of electrode materials, such as carbon materials [3, 4], transition metal oxides [5-8], and conducting polymers [9, 10], are studied to applied in supercapacitors. Among electrode materials, transition metal oxides possess higher energy density than carbon materials and better cycle life than conducting polymers. Recently, mixed transition metal oxides, such as $NiCo_2O_4$ [11-13], $MnCo_2O_4$ [14], $CoFe_2O_4$ [15], $NiMn_2O_4$ [16], and $ZnCo_2O_4$ [17], have been applied in supercapacitors because they can provide higher capacitive property than corresponding monometal

oxides. Among mixed transition metal oxides, manganese-cobalt oxides, such as $MnCo_2O_4$ and $MnCo_2O_{4.5}$, have received attention because of their natural abundance, inexpensive cost, environmental benignity, and large theoretical capacitance [18]. There are a certain number of papers on $MnCo_2O_4$ electrode material for supercapacitors. However, $MnCo_2O_{4.5}$ electrode material for supercapacitors is rarely researched. For example, a specific capacitance of 151.2 F g^{-1} at 5 mV s^{-1} was obtained for porous urchin-like $MnCo_2O_{4.5}$ hierarchical architectures studied by Li et al. [19]. Wang et al. [20] synthesized $MnCo_2O_{4.5}$ nanoparticles, which exhibits a specific capacitance of 158 F g^{-1} at 5 mV s^{-1}. In their researches, the specific capacitance of $MnCo_2O_{4.5}$ electrode material was relatively low because of low electronic conductivity of $MnCo_2O_{4.5}$ like other monometal oxides. In order to improve its specific capacitance, a viable way is to form composite with carbon materials with good electronic conductivity. Among carbon materials, graphene is attractive because of its excellent electronic conductivity, high specific surface area, and chemical stability [21].

Al-Rubaye et al. [18] syethesized $MnCo_2O_4$/graphene composite as electrode material for supercapacitors. However, $MnCo_2O_4$/graphene composite was prepared by complicated multistep processes, which involved the formation of $MnCo_2O_4$ via a hydrothermal technique accompanying subsequently calcination and the preparation of $MnCo_2O_4$/graphene composite with an electrophoretic deposition technique. Moreover, $MnCo_2O_4$/graphene composite instead of $MnCo_2O_{4.5}$/graphene composite was synthesized to employ as electrode material for supercapacitors. In the present work, $MnCo_2O_{4.5}$/graphene composite was prepared by a facile hydrothermal process. As a result, $MnCo_2O_{4.5}$/graphene composite as supercapacitors electrode material shows high specific capacitance, good rate capability and excellent cycling stability. Up to now, there are few reports about $MnCo_2O_{4.5}$/graphene composite as electrode material for supercapacitors.

2. EXPERIMENTAL

2.1. Synthesis of $MnCo_2O_4$/graphene Composite

$MnCo_2O_4$/graphene composite was prepared by a hydrothermal process. In a typical procedure, 80 mg of graphite oxide was dispersed in 25 mL deionized water with sonication. Afterwards, 0.245 g of $Mn(AC)_2{\cdot}4H_2O$, 0.582 g of $Co(NO_3)_2{\cdot}6H_2O$, 0.9 g of $CO(NH_2)_2$, 0.222 g of NH_4F were added into the above solution and continually stirred to form a mixed solution. The mixed solution was then transferred into a Teflon-lined stainless steel autoclave. Subsequently, the stainless steel autoclave was sealed and hydrothermally treated at 150 ℃ for 16 h. After naturally cooled to room temperature, the obtained precipitate was alternately centrifuged and washed three times with deionized water and ethanol. Finally, precipitate was dried at 60 ℃ for 12 h and then annealed in a muffle furnace at 350 ℃ for 3 h to obtain $MnCo_2O_4$/graphene composite.

2.2. Materials Characterization

The structure of $MnCo_2O_4$/graphene composite was characterized by X-ray diffraction (XRD, Bruker, D8-Advance) with Cu Kα radiation, scan range from 10° to 80°. The morphology of $MnCo_2O_4$/graphene composite was analyzed by scanning electron microscopy (FEI Nova Nano-230).

2.3. Electrochemical Test

The synthesized $MnCo_2O_4$/graphene composite (80 wt %), conductive agent (acetylene black, 15 wt) and binder (polytetrafluoroethylene, 5 wt %) were first mixed. Then, the mixture was coated on a nickel foam (1 cm × 1cm), dried naturally and pressed at 10 Mpa. Finally, the working electrode was prepared by drying at 110 °C for 12 h under vacuum. The capacitive behavior of the sample was tested with a CHI 660E electrochemical workstation (Shanghai, China). Cyclic voltammetry (CV), galvanostatic charge-discharge (GCD) and electrochemical impedance spectroscopy (EIS) measurements were carried out using a three-electrode configuration at room temperature. A Pt plate was used as the counter electrode, and all potential are referred to a saturated calomel electrode (SCE) reference electrode. 2 M KOH solution was used to the electrolyte. EIS measurements were conducted between 0.01 and 10^5 Hz.

3. RESULTS AND DISCUSSION

3.1. XRD analyses

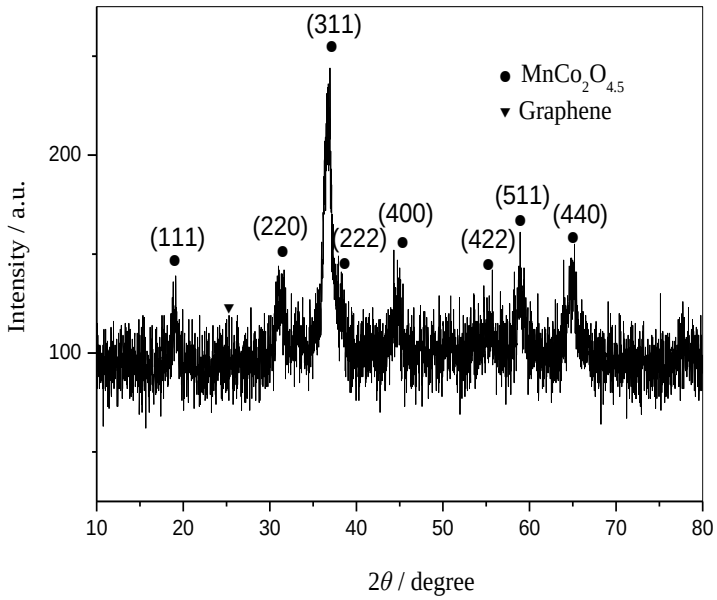

Figure 1. XRD pattern of $MnCo_2O_{4.5}$/graphene composite.

Fig. 1 shows XRD pattern of $MnCo_2O_{4.5}$/graphene composite. The XRD peaks at 2θ locating at 19.0°, 31.2°, 36.8°, 38.5°, 44.8°, 55.8°, 58.9° and 65.2° are assigned to the (111), (220), (311), (222), (400), (422), (511) and (440) crystal planes of $MnCo_2O_{4.5}$ (JCPDS No. 32-0297, a=b=c=8.08 Å), respectively. The peak at 2θ locating at 26.3° is attributed to the (002) crystal plane of graphene [21-23]. No other peaks are detected in the XRD patterns, indicating that the sample consists of $MnCo_2O_{4.5}$ and graphene.

3.2. Morphology

The low magnification and high magnification SEM images of $MnCo_2O_{4.5}$/graphene composite are displayed in Fig. 2a and 2b, respectively. Crumpled structure is graphene in the composite and cracked ellipsoidal-like microstructure composed of agglomerated nanoparticles is $MnCo_2O_{4.5}$ in the composite. Besides, under the high magnification (Fig. 2b), the morphology of $MnCo_2O_{4.5}$ in $MnCo_2O_{4.5}$/graphene composite clearly shows that the surface of cracked ellipsoidal-like microstructure is coarse and exists interspaces.

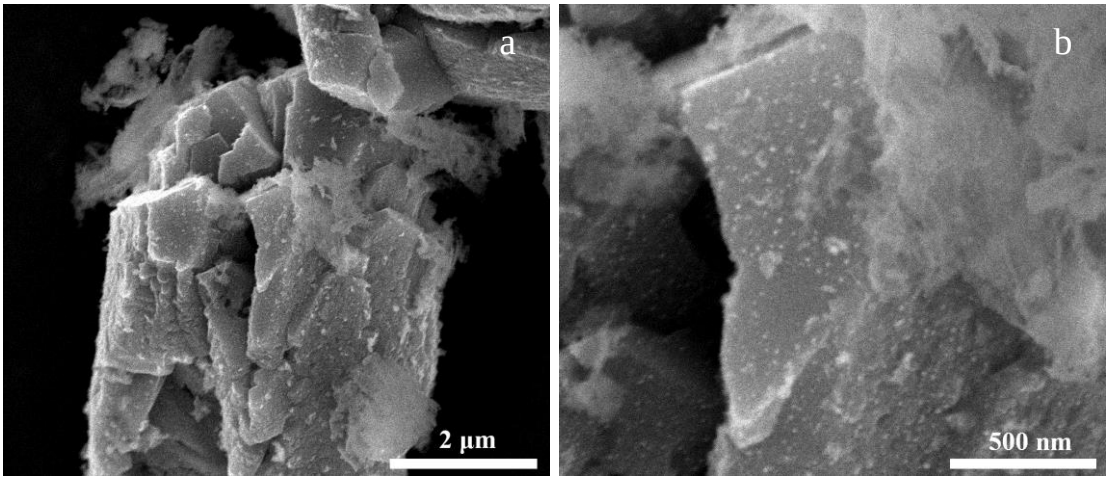

Figure 2. SEM images of $MnCo_2O_{4.5}$/graphene composite: (a) low magnification; (b) high magnification.

Interspaces in cracked ellipsoidal-like microstructure can benefit the penetration of the electrolyte. Coarse surface of cracked ellipsoidal-like microstructure possesses high specific surface area. Therefore, these microstructure of $MnCo_2O_{4.5}$ in $MnCo_2O_{4.5}$/graphene may be in favor of enhancing capacitive properties of material [24, 25].

3.3. Electrochemical capacitor property

Cyclic voltammograms of $MnCo_2O_{4.5}$/graphene composite electrode within a potential window -0.2-0.6 V at different scan rates are shown in Fig. 3a.

The shape of the CV curves is not an ideal rectangular shape but exhibits obvious redox couple peaks in the potential windows, which signifies that capacitance largely originates from pseudo-capacitance caused by faradaic redox reactions. The shape of the CV curves also exhibits excellent symmetry, implying the electrochemical reversibility of faradic redox reactions. The peak current density and enclosed area become large when the scan rate increases. Futhermore, the anodic and cathodic peaks are observed to shift to negative and positive potentials as the scan rate increases, respectively. This may be ascribable to the limited diffusion time [26]. Noteworthily, the redox peaks also appeares when the scan rate increses to a high value (80 mV s^{-1}), suggesting that the

$MnCo_2O_{4.5}$/graphene composite is beneficial to fast redox reaction [27, 28]. The average specific capacitance of $MnCo_2O_{4.5}$/graphene composite can be calculated from the CV curves as follows [29-31]:

$$C_{sp} = \frac{1}{mv(V_a - V_c)} \int_{V_a}^{V_c} I(V)dV \quad (1)$$

where C_{sp} is the specific capacitance (F g^{-1}), I is the current (A), v is the scan rate (mV s^{-1}), V_a is the lowest potential (V), V_c is the highest potential (V), m represents the mass of $MnCo_2O_{4.5}$/graphene composite (g). Based on the formula (1), the specific capacitance of $MnCo_2O_{4.5}$/graphene composite eledtrode at various scan rate is displayed in Fig. 3b. As shown in Fig. 3b, $MnCo_2O_{4.5}$/graphene composite possesses a C_{sp} of 255.8 F g^{-1} at 5 mV s^{-1}, which is much better than those of $MnCo_2O_{4.5}$ as electrode materials for supercapacitors studied by Li et al. (151.2 F g^{-1} at 5 mV s^{-1}) [19] and Wang et al. (158 F g^{-1} at 5 mV s^{-1}) [20] (Table 1). As the scan rate increase, the specific capacitance drops. However, the specific capacitance still remains 176.7 F g^{-1} at 80 mV s^{-1}. A specific capacitance retention of 69.1% for a 16-time scan rate increase is obtained. It implies relatively high specific capacitance and good rate capability of $MnCo_2O_{4.5}$/graphene composite.

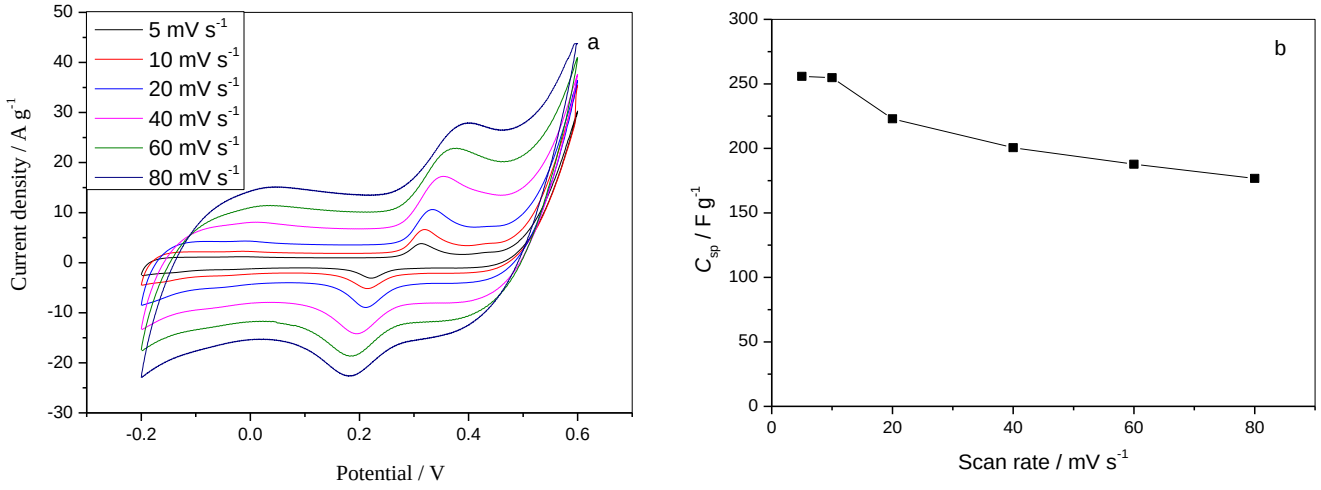

Figure 3. Cyclic voltammograms of $MnCo_2O_{4.5}$/graphene composite eledtrode within a potential window -0.2-0.6 V at scan rates of 5, 10, 20, 40, 60 and 80 mV s^{-1} (a); The specific capacitance of $MnCo_2O_{4.5}$/graphene composite eledtrode at scan rates of 5, 10, 20, 40, 60 and 80 mV s^{-1} (b).

Fig. 4 depicts galvanostatic charge–discharge curves of $MnCo_2O_{4.5}$/graphene composite electrode at the current densities of 0.5, 1, 2, 4 and 8 A g^{-1}. Apparently, nonlinearity in the charge-discharge curves is observed, which further verifies the pseudocapacitive characteristics caused by faradaic reactions. This is in accordance with the results of the CV curves. The specific capacitance of $MnCo_2O_{4.5}$/graphene composite can be calculated as follows [1, 32-34].

$$C_{sp} = \frac{It}{mV} \quad (2)$$

where C_{sp} is the specific capacitance (F g^{-1}), I represents the discharge current (A), t indicates the discharge time (s), V is the discharge potential window, m is the mass of active material, respectively. On basis of the formula (2), the specific capacitance of electrode at different current densities is displayed in Fig. 5. Obviously, the specific capacitance gradually decreases with increasement of the current density.

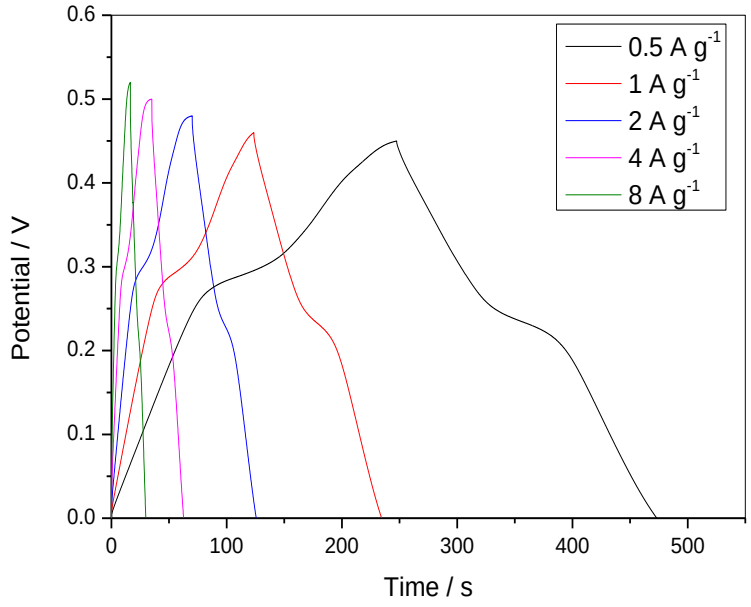

Figure 4. Galvanostatic charge-discharge curves of $MnCo_2O_{4.5}$/graphene composite eledtrode at the current densities of 0.5, 1, 2, 4 and 8 A g^{-1}.

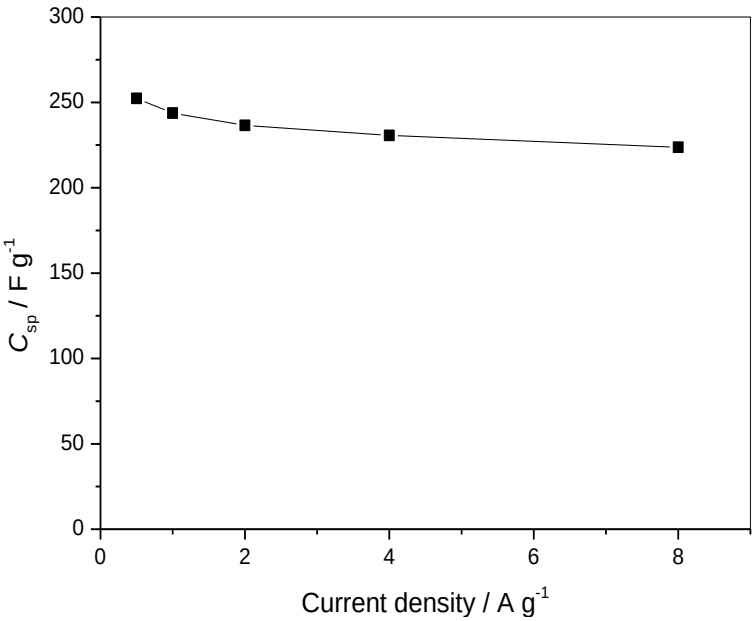

Figure 5. The specific capacitance of $MnCo_2O_{4.5}$/graphene composite eledtrode at the current densities of 0.5, 1, 2, 4 and 8 A g^{-1}.

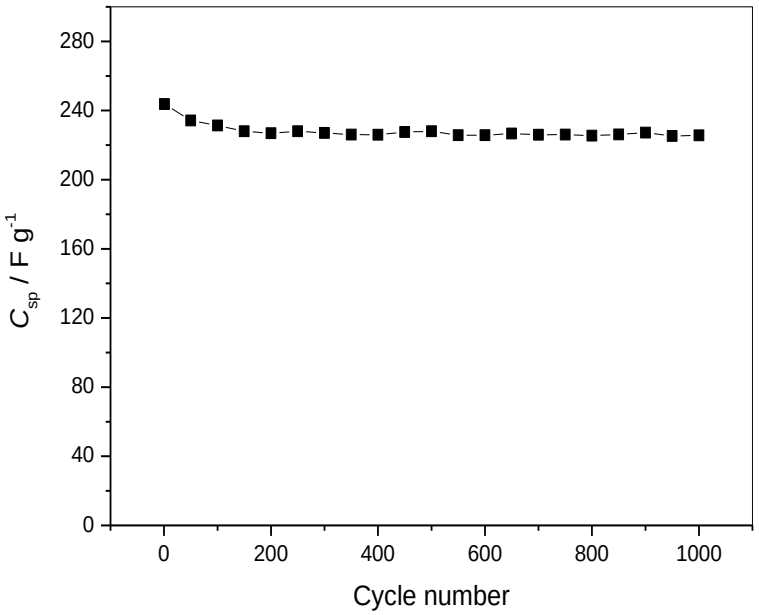

Figure 6. Cycling performance of $MnCo_2O_{4.5}$/graphene composite eledtrode at the current density of 1 A g^{-1}.

The specific capacitance of $MnCo_2O_{4.5}$/graphene composite at 0.5 A g^{-1} is calculated to be 252.3 F g^{-1}, which is much higher than previous work reported by Li et al. (122.4 F g^{-1} at 0.5 A g^{-1}) [19] and Wang et al. (144 F g^{-1} at 0.5 A g^{-1}) [20] (Table 1). The main reason for the above behavior is ascribable to synergistic effect between $MnCo_2O_{4.5}$ and graphene. A specific capacitance of 223.7 F g^{-1} is obtained at 8.0 A g^{-1}. 88.7% of the specific capacitance is retained for a 16-time increase in the current density, indicating that $MnCo_2O_{4.5}$/graphene composite possess superior rate capability. The results are in accordance with those calculated from the CV curves.

Table 1. Comparision of the specific capacitance reported in the references with this study for $MnCo_2O_{4.5}$ (or $MnCo_2O_{4.5}$/graphene)

Synthesis method	Materials	Electrolyte	Current density or scan rate	Specific capacitance	Reference
Hydrothermal	$MnCo_2O_{4.5}$	1 M KOH	5 mV s^{-1}	151.2 F g^{-1}	[19]
			0.5 A g^{-1}	122.4 F g^{-1}	
Chemical transformation	$MnCo_2O_{4.5}$	1 M Na_2SO_4	5 mV s^{-1}	158 F g^{-1}	[20]
			0.5 A g^{-1}	144 F g^{-1}	
Hydrothermal	$MnCo_2O_{4.5}$/graphene	2 M KOH	5 mV s^{-1}	255.8 F g^{-1}	This work
			0.5 A g^{-1}	252.3 F g^{-1}	

Fig. 6 dispalys cycling performance of $MnCo_2O_{4.5}$/graphene composite eledtrode at the current density of 1 A g^{-1}. The specific capacitance slightly drops to 231.1 F g^{-1} at the 100th cycle and then nearly keeps stable when increases the cycle number. At the 1000th cycle, the specific capacitance is

calculated to be 225.6 F g^{-1}, which is 92.6% of initial specific capacitance (243.7 F g^{-1} at 1 A g^{-1}). The results indicate that $MnCo_2O_{4.5}$/graphene composite has excellent cycling stability.

Fig. 7a demonstrates Nyquist impedance plots of $MnCo_2O_{4.5}$/graphene composite electrode measured at 0.1 V. Fig. 7b shows the equivalent circuit for modeling Nyquist plots.

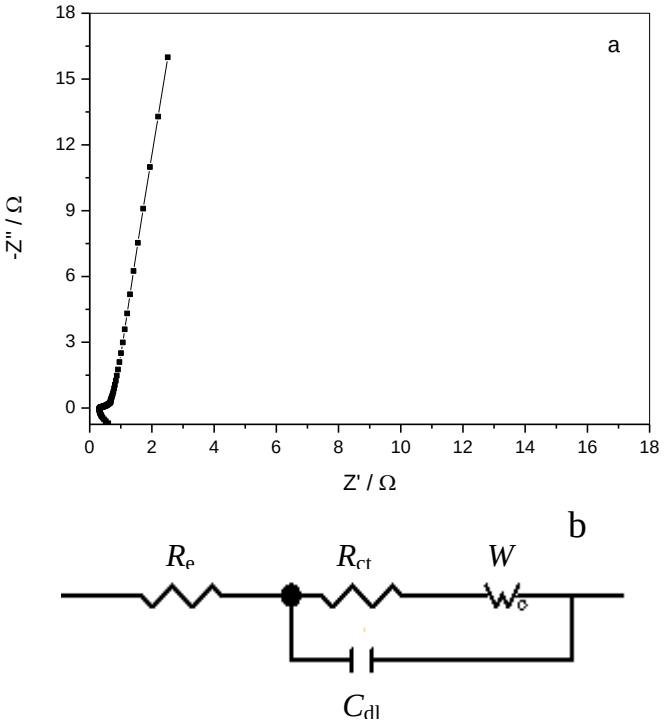

Figure 7. Nyquist impedance plots of $MnCo_2O_{4.5}$/graphene composite electrode measured at 0.1 V (a); The equivalent circuit for modeling Nyquist plots (b).

Nyquist plots contain a incomplete small semicircle in the high frequency range and a straight line in the low frequency range. The point intersecting at the real axis in the high frequency range represents a combinational resistance (R_e), which contains the active material intrinsic resistance, the electrolyte resistance, and contact resistance at the active material/the current collector interface [35]. R_e is around 0.32 Ω, which is very low. This is attributable to excellent electron conductivity provided by graphene in $MnCo_2O_{4.5}$/graphene composite. A semicircle in the high frequency region corresponds to the charge-transfer resistance (R_{ct}) and the double-layer capacitance [24, 30, 36]. The charge-transfer resistance (R_{ct}) is ca. 0.05 Ω. The low R_{ct} value signifies good charge-transfer kinetics and easy electron transport between the electrolyte and the electrode, resulting in good rate capability of $MnCo_2O_{4.5}$/graphene composite [37]. In the low frequency range, the straight line corresponds to the diffusive resistance (Warburg impendence, W) of the electrolyte ions in electrode. The slope of the straight line tends to vertical asymptote, indicating that $MnCo_2O_{4.5}$/graphene composite possesses a good capacitive behavior [24, 30, 38].

4. CONCLUSIONS

$MnCo_2O_{4.5}$/graphene composite is obtained by hydrothermal process and its capacitive performance is investigated. $MnCo_2O_{4.5}$/graphene composite possesses a specific capacitance of 255.8 F g^{-1} at 5 mV s^{-1} and a specific capacitance of 176.7 F g^{-1} at 80 mV s^{-1}. Its specific capacitance is 252.3 and 223.7 F g^{-1} at 0.5 and 8.0 A g^{-1}, respectively. The specific capacitance retention ratio for a 16-time scan rate increase and a 16-time current density increase are 69.1% and 88.7%, respectively, indicating its superior rate capability. The specific capacitance after 1000 cycles is 225.6 F g^{-1} at 1.0 A g^{-1} and 92.6% of initial specific capacitance is achieved, demonstrating relative good cycling stability of $MnCo_2O_{4.5}$/graphene composite. All the results indicate $MnCo_2O_{4.5}$/graphene composite as supercapacitors electrode material with high specific capacitance, good rate capability and excellent cycling stability.

ACKNOWLEDGEMENTS
This work was financially supported by Scientific Research Fund of Hunan Provincial Education Department (No. 14B022), Science and Technology Plan Fund of Changsha (No. k1509008-11) and Aid Program for Science and Technology Innovative Research Team in Higher Educational Institutions of Hunan Province.

References

1. Y.H. Li, K.L. Huang, D.M. Zeng, S.Q. Liu and Z.F. Yao, *J. Solid State Electrochem.*, 14 (2010) 1205.
2. Q. Wang, J. Yan and Z.J. Fan, *Energy Environ. Sci.*, 9 (2016) 729.
3. Y.F. Song, J. Yang, K. Wang, S. Haller, Y.G. Wang, C.X. Wang and Y.Y. Xia, *Carbon*, 96 (2016) 955.
4. F. Bonaccorso, L. Colombo, G. Yu, M. Stoller, V. Tozzini, A.C. Ferrari, R.S. Ruoff and V. Pellegrini, *Science*, 347 (2015) 1246501.
5. S. Bag and C.R. Raj, *J. Mater. Chem. A*, 4 (2016) 587.
6. C.H. Zhao, B.Y. Huang, W.B. Fu, J.Y. Chen, J.Y. Zhou and E.Q. Xie, *Electrochim. Acta*, 178 (2015) 555.
7. Y.B. Zhang and Z.G. Guo, *Chem. Commun.*, 50 (2014) 3443.
8. Z.S. Iro, C. Subramani and S.S. Dash, *Int. J. Electrochem. Sci.*, 11 (2016) 10628.
9. K. Wang, H.P. Wu, Y.N. Meng and Z.X. Wei, *Small*, 10 (2014) 14.
10. P. Sekar, B. Anothumakkool, V. Vijayakumar, A. Lohgaonkar and S. Kurungot, *Chemelectrochem*, 3 (2016) 933.
11. R.J. Deokate, R.S. Kalubarme, C.-J. Park and C.D. Lokhande, *Electrochim. Acta*, 224 (2017) 378.
12. Y.R. Zhu, J.F. Wang, Z.B. Wu, M.J. Jing, H.S. Hou, X.N. Jia and X.B. Ji, *J. Power Sources*, 287 (2015) 307.
13. S. Khalid, C.B. Cao, A. Ahmad, L. Wang, M. Tanveer, I. Aslam, M. Tahir, F. Idrees and Y.Q. Zhu, *Rsc Advances*, 5 (2015) 33146.
14. V. Venkatachalam, A. Alsalme, A. Alghamdi and R. Jayavel, *J. Electroanal. Chem.*, 756 (2015) 94.
15. Z. Wang, W. Jia, M. Jiang, C. Chen and Y. Li, *Nano Research*, 9 (2016) 2026.
16. K.V. Sankar, S. Surendran, K. Pandi, A.M. Allin, V.D. Nithya, Y.S. Lee and R.K. Selvan, *Rsc Advances*, 5 (2015) 27649.
17. H. Wu, Z. Lou, H. Yang and G.Z. Shen, *Nanoscale*, 7 (2015) 1921.

18. S. Al-Rubaye, R. Rajagopalan, C.M. Subramaniyam, Z. Yu, S.X. Dou and Z. Cheng, *J. Power Sources*, 324 (2016) 179.
19. W.Y. Li, K.B. Xu, G.S. Song, X.Y. Zhou, R.J. Zou, J.M. Yang, Z.G. Chen and J.Q. Hu, *CrystEngComm*, 16 (2014) 2335.
20. K. Wang, J. Xu, A. Lu, Y. Shi and Z. Lin, *Solid State Sci.*, 58 (2016) 70.
21. Y.H. Li, S.Y. Zhang, Q.Y. Chen and J.B. Jiang, *Int. J. Electrochem. Sci.*, 10 (2015) 6199.
22. D.H. Zhang and W.B. Zou, *Curr. Appl. Phys.*, 13 (2013) 1796.
23. Y.H. Li, J.B. Li, S.Y. Zhang, N.F. Wang and Z. Zhou, *Int. J. Electrochem. Sci.*, 10 (2015) 8005.
24. Y.H. Li, K.L. Huang, Z.F. Yao, S.Q. Liu and X.X. Qing, *Electrochim. Acta*, 56 (2011) 2140.
25. F.Z. Deng, L. Yu, G. Cheng, T. Lin, M. Sun, F. Ye and Y.F. Li, *J. Power Sources*, 251 (2014) 202.
26. B.R. Duan and Q. Cao, *Electrochim. Acta*, 64 (2012) 154.
27. L.L. Zhang, X. Zhang, L. Pei, Y.J. Zhang and Y.D. Xu, *Mater. Lett.*, 164 (2016) 333.
28. J. Pu, Z.H. Wang, K.L. Wu, N. Yu and E.H. Sheng, *Phys. Chem. Chem. Phys.*, 16 (2014) 785.
29. H. Li, S. Liu, C. Huang, Z. Zhou, Y. Li and D. Fang, *Electrochim. Acta*, 58 (2011) 89.
30. H.Y. Quan, B.C. Cheng, Y.H. Xiao and S.J. Lei, *Chem. Eng. J.*, 286 (2016) 165.
31. H.B. Li, M.H. Yu, F.X. Wang, P. Liu, Y. Liang, J. Xiao, C.X. Wang, Y.X. Tong and G.W. Yang, *Nature Communications*, 4 (2013) 1894.
32. X. Yu, B. Lu and Z. Xu, *Adv. Mater.*, 26 (2014) 1044.
33. Y.H. Li, K.L. Huang, S.Q. Liu, Z.F. Yao and S.X. Zhuang, *J. Solid State Electrochem.*, 15 (2011) 587.
34. Y.H. Li and Q.Y. Chen, *Asian J. Chem.*, 24 (2012) 4736.
35. W.L. Yang, Z. Gao, J. Ma, J. Wang, B. Wang and L.H. Liu, *Electrochim. Acta*, 112 (2013) 378.
36. Q. Guan, J.L. Cheng, B. Wang, W. Ni, G.F. Gu, X.D. Li, L. Huang, G.C. Yang and F.D. Nie, *ACS Appl. Mater. Interfaces*, 6 (2014) 7626.
37. H. Che, A. Liu, J. Mu, Y. Bai, C. Wu, X. Zhang, Z. Zhang and G. Wang, *Electrochim. Acta*, 225 (2017) 283.
38. H.F. An, Y. Wang, X.Y. Wang, N. Li and L.P. Zheng, *J. Solid State Electrochem.*, 14 (2010) 651